EFFECTS OF NUMBER OF TURNS OF ARMATURE WINDING ON OUTER ROTOR BRUSHLESS DIRECT CURRENT MOTOR DESIGNED FOR AN ELECTRIC VEHICLE PROTOTYPE

Alper Sefa ÇAĞIŞLAR[1] iD **, Hasan TİRYAKİ[2,*]** iD **, Nevra BAYHAN[3]** iD

[1,2,3]*Istanbul University - Cerrahpaşa, Electrical and Electronics Engineering Department, 34320, Istanbul, Turkey*

ABSTRACT

While electric vehicles happen to be today's transportation vehicles, big R&D investments are being made by automobile manufacturers. Outer and inner rotor motors are used for electric vehicles. Considering the fact that the transmission systems make the structure more complex, outer rotor motors come into prominence in applications requiring small power. This study includes the design of outer rotor brushless direct current motor for electric vehicle prototypes. In addition, the effects of the number of turns of the armature winding selected, especially on efficiency, input power and torque parameters, were analyzed in detail.

Keywords: Brushless direct current motor, Design, Turns, Efficiency, Power, Torque

ARMATÜR SARGISININ SARIM SAYISININ BİR ELEKTRİKLİ ARAÇ PROTOTİPİ İÇİN TASARLANAN DIŞ ROTORLU FIRÇASIZ DOĞRU AKIM MOTORUNA ETKİLERİ

ÖZET

Elektrikli araçlar günümüzün ulaşım araçları olarak yerini alırken otomobil üreticileri tarafından bu konuda büyük Ar-Ge yatırımları yapılmaktadır. Elektrikli araçlar için dışsal ve içsel rotorlu motorlar kullanılmaktadır. Aktarım organlarının yapıyı daha karmaşıklaştırdığı göz önünde bulundurulduğunda dışsal rotorlu motorlar küçük güç gerektiren uygulamalarda verimlilikleri ile ön plana çıkmaktadır. Bu çalışma prototip elektrikli araçlar için dış rotorlu fırçasız doğru akım motoru tasarımını içermektedir. Ayrıca yapılan analizler ile seçilen armatür sargısının sarım sayısının özellikle verimlilik, giriş gücü ve tork parametrelerine olan etkileri detaylı olarak incelenmiştir.

Anahtar kelimeler: Fırçasız doğru akım motoru, Tasarım, Sarım sayısı, Verimlilik, Güç, Moment

1. INTRODUCTION

The transportation sector continues to evolve in different ways with today's technology. High-efficiency electric vehicles, which are increasing in use and which do not harm the environment, are being preferred by the technology developing day by day. Electric cars, motorcycles, skateboards and many other technological vehicles are attracting worldwide attention and are moving rapidly towards becoming the indispensable technology of the future. The motor to be selected under all these conditions is really important.

Direct current motors are widely used in industrial applications. Limited use of brushed models in some areas has enabled Brushless DC motors to stand out. Need for continuous maintenance of brushed-type motors provides disadvantage in variable conditions and in the areas of continuous use. For this reason, brushless DC motors have a wide range of applications. Brushless DC motors come to the forefront with performance values such as high efficiency and high torque.

Direct current motors are motors in which the magnetic field is produced by means of magnets. The magnet can be an electromagnet or a permanent magnet. When a permanent magnet is used to create a magnetic field in a direct current motor, the motor is called a permanent magnet direct current motor or a permanent magnet brushless direct current (BLDC) motor [1].

Brushless direct current motor is in fact configured as a rotating magnet through a series of coil-carrying conductors. Current in the conductors and the magnets that are arranged in order for the torque to be in one direction need to be positively positioned

A. S. Çağışlar, H. Tiryaki, N. Bayhan

as the rotation takes place. Direct current is carried out by the pole switching commutator and brushes in commutator motor. Since the commutator is fixed to the rotor, switching events are automatically synchronized with the alternating polarity of the magnetic field through which the conductors pass. Polarity of the brushless DC motor is carried out by the power transistors which must be switched in synchronous with the rotor position. The commutation process is similar in two machines, and the resulting performance equations and speed / torque concepts are almost identical.

Brushless DC motors with outer rotor type are used for applications requiring high torque and inertia. This type of motors are used in many areas such as vehicle wiper motor, automatic windows, robotic, generator, electric vehicles, unmanned aerial vehicles, white goods sector [2]. Although there are various disadvantages such as motor protection and resistance to shocks in outer rotor applications, it is preferable that applications do not need any transfer components because they provide direct drive of the moment. In addition, the motor drives used for brushless DC motors have a more complex structure than other motors. Due to the high torque values of outer rotor brushless direct current motors, they are used in electric vehicles in particular [3].

Rahim et al. have designed a brushless direct current motor design and prototype manufacturing for electric vehicles with a weight of less than 150 kg, operating in axial structure at 300V high voltage and small in volume [4].

Shrivastava and Brahmin have designed a outer rotor brushless direct current motor in two different three-phase slot / pole combinations for use in electric vehicle applications, and examined the design results. The motor design they have made is a motor that operates at 300V high voltage and is large in volume [5].

Durmus and Solmaz, similar to the activities carried out in this study, have performed a brushless DC motor design and finite element analysis with typical methods. In their study, an motor design, which operates at 60V voltage, 1100 rpm, but cannot provide sufficient power and torque values for passenger cars, has been obtained. Torque charts, flux lines, speed and efficiency parameters were examined in finite element analysis of the resulting motor design and they suggested the use of the motor in hybrid cars that can operate in parallel structure [6].

In the electric vehicle prototypes, direct drive brushless direct current motors are preferred due to their higher efficiency. However, in order to keep efficiency in the maximum range, the motors must be designed and manufactured in accordance with the vehicle and its features. It is very important to determine the correct number of turns of armature winding, as well as many parameters during the design phase.

In this study, an outer rotor brushless DC motor is designed for an electric vehicle prototype. While designing, the effects of the number of turns of armature winding used in the desired speed ranges on the efficiency, power and torque parameters to be considered in the design of the brushless DC motor are examined comparatively and the optimal number of turns of armature winding has been determined for design.

2. MATERIALS AND METHODS

Since the effects of the number of turns of armature winding to be used in this study will be examined in the motor design, a detailed study has been done in this section. The other parameters are described below.

2.1. Determination of Power and Torque Parameters for Motor Design

The motor to be designed will be the BLDC motor with outer rotor. In the case of outer rotor motor applications, a design can be realized without the need of any transferring systems and ignoring the losses of this transfer organ. The greatest advantage of these motors is the direct transfer of torque [7]. Figure 1 shows the forces affecting the vehicle.
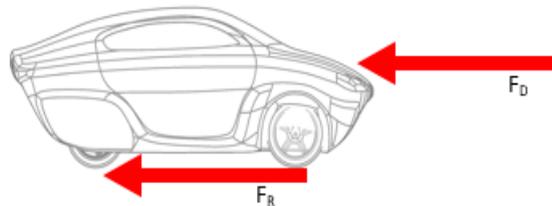
Figure 1. The forces affecting the vehicle.

Design requirements for the outer BLDC can be defined using following equations:

$$F_D = \frac{1}{2}\rho v^2 A C_D \tag{1}$$

EFFECTS OF NUMBER OF TURNS OF ARMATURE WINDING ON OUTER ROTOR BRUSHLESS DIRECT CURRENT MOTOR DESIGNED FOR AN ELECTRIC VEHICLE PROTOTYPE

Drag Force (DF) formed by air on an object is shown in (1). F_D drag force, ρ air density, v object velocity, A is the object's cross-sectional surface area and C_D is the object's aerodynamic friction coefficient.

Another force to be calculated for the vehicle is the Rolling Resistance Force (RRF).

$$F_R = f_s mg \tag{2}$$

where F_R is defined as friction force. f_s is the coefficient of friction of the tire used and g is the force of gravity.

The forces of F_D and F_R, which constitute the fundamental forces of the vehicle, are involved in the determination of torque and power requirements as motor parameters. Considering Figure 1, the necessary moment calculations related to these forces are calculated by considering the force and force arm rule.

$$\tau_D = F_D r_D \tag{3}$$

The amount of torque required to resist wind is given in (3). τ_D represents the amount of torque required and r_D represents the distance from the center of the surface density center of the vehicle to the center of the wheel.

$$\tau_R = F_R r_R \tag{4}$$

The required torque calculation against rolling resistance is given in (4). τ_R represents the amount of torque required and the distance between the r_R ground and the center of the wheel.

$$\tau_{motor} = \tau_D + \tau_R \tag{5}$$

When (3) and (4) are combined, the amount of torque that the motor must produce at a certain speed, as in (5), arises.

$$w_{rpm} = \frac{1000v}{60.2\pi R} \tag{6}$$

(6) represents the speed of the w_{rpm} wheel in rpm. v is the radius of the wheel in km / h as speed and R meter.

$$w_{motor} = \frac{2\pi \, w_{rpm}}{60} \tag{7}$$

In (7), w_{motor} as an angular velocity its in radial/sec.

$$P_{motor} = \tau_{motor} w_{motor} \tag{8}$$

In the light of the necessary calculations, the equation of power in (8), which we can describe in general, emerges. P_{motor} refers to the rated power of the motor [7].

The parameters of the vehicle to be applied should be determined within the framework of high engineering and analysis. The vehicle planned to be implemented is the AZAK prototype electric racing vehicle produced by the MilAT 1453 R&D Society and the most efficient vehicle record ever made in the Alternative Energy Vehicle Races organized by the TUBITAK.

The information about the AZAK vehicle, which has been produced by the Department of Electrical and Electronics Engineering, Istanbul University - Cerrahpasa, is given in Table 1.

Table 1. Parameters of the vehicle AZAK

VEHICLE INFORMATION	VALUES
Reference velocity	$v = 56 \ km/h = 15.51 \ m/sn$
Weight of the vehicle	$m = 215 \ kg$
Radius of the tire used	$R = 0.279 \ metre$
Friction Coef. Of the tire used	$C = 0.009$
Front surface of the vehicle subject to friction	$A = 1.18 \ m^2$
Friction coefficient of the vehicle (The result of aerodynamic analysis)	$C_D = 0.07$
Air Density	$\rho = 1.225 \ kg/m^3$
The distance from the center of the vertical section of the vehicle to the wheel hub	$r_D = 0.32 \ metre$

A. S. Çağışlar, H. Tiryaki, N. Bayhan

Depending on motor usage and load, varying power and torque values must be determined [3]. Calculations according to the weight of the vehicle to be used and the speed required to determine the nominal values are described above.

The nominal speed of the motor to be used for the electric vehicle varies depending on the wheel diameter and the rated speed. 56 km/hour value is calculated for the vehicle planned to be done and the number of rotations were determined. The calculations were made assuming that the forces to be defeated were DF and RRF.

As shown in Table 2, the torque required to move the BLDC motor at 56 km/h was 9.2Nm and the rated power was 512.9W.

The torque required to reach a speed of 56 km / h in 30 seconds is set at 28.93 Nm and the maximum power required is approximately 1.5 kW [8].

Table 2. Calculated design values

Calculated Values	Results
Drag Force	$F_D = 12.17 N$
Rolling Resistance Force	$F_R = 18.98 N$
Acceleration Force	$Fm = 94 N$
Total Needed Torque	$\tau_{motor} = 9.2 Nm$
Revolution of Tires	$w_{rpm} = 532.42 d/d$
Angular Speed	$w_{motor} = 55.75 rad/sn$
Nominal Power	$P_{motor} = 512.9 W$

2.2. Determination of Battery Voltage

One of the features that should be determined during the design phase is the determination of the slot-pole combination of the motor. This parameter fundamentally affects the stator and rotor design of the motor.

Increasing the number of poles means increasing the number of magnets, which increases the torque generated. When the studies corresponding to the number of slots corresponding to the number of poles are examined, the winding factor should be considered [9].

The winding factor is calculated using electromotive force phasors. For this purpose, the number of poles and slots of the motor with winding factor must be determined [10]. Battery features are given in Table 3.

Table 3. Battery features

Features	Values
Operating voltage	48 V
Parallel Number	12
Serial Number	12
Total Power	1632 Watt

2.3. Determination of Slot-Pole Combination

One of the features that should be determined during the design phase is the determination of the slot-pole combination of the motor. This parameter fundamentally affects the stator and rotor design of the motor.

When the studies corresponding to the number of slots corresponding to the number of poles are examined, the winding factor should be considered [9].

The image of the relative angular deviation of the coils of the motor is shown in Figure 2.
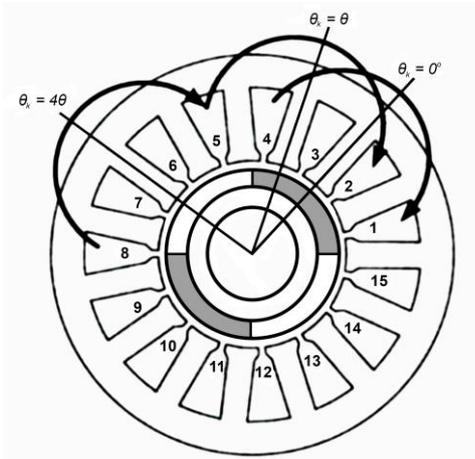
The expression of the angle is as in (9).

$$\theta_k = (k-1)\frac{N_m}{N_s}180°E \tag{9}$$

θ_k, refers to the relative angular deviation of coil k. N_m is shown as the number of poles and N_s is the number of slots.

$$K_{wn} = \frac{1}{N_{cph}}\sum_{k=1}^{N_{cph}} e^{-jn\theta_k} \tag{10}$$

EFFECTS OF NUMBER OF TURNS OF ARMATURE WINDING ON OUTER ROTOR BRUSHLESS DIRECT CURRENT MOTOR DESIGNED FOR AN ELECTRIC VEHICLE PROTOTYPE

(10) is the equation of the winding factor. Here the K_{wn} represents winding factor, N_{cph} is the number of slots per phase. n is the harmonic index, and θ is the relative angular deviation of the coil k [1].

Figure 2. Motor with four poles and fifteen slots [1].

Figure 3. Winding factor values corresponding to the slot-pole combination [1].

The winding factor responses corresponding to the slot-pole combinations are shown in Figure 3. k_{w1} refers to the first harmonic winding factor. The winding factor refers to the ability of the electrical power applied to the motor to be converted to torque [11].

The values shown in Figure 4 affects the determination of the output power, operating temperature, slot fill factor and air gap constant determined at the beginning of the design [12].

As described below, a slot-pole combination should be chosen to keep the winding factor high [13]. In terms of cost, it is aimed to provide the need of application with high power density by making a selection that keeps the number of permanent magnets higher, since there is no obstacle in the prototype based studies.

A. S. Çağışlar, H. Tiryaki, N. Bayhan
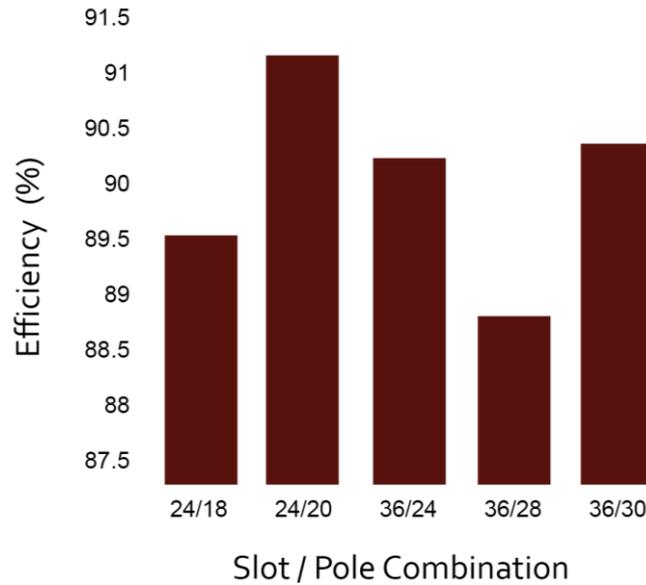
**Figure 4.** The effect of slot-pole combination on maximum efficiency [14].

The slot-pole combination was determined as 36/32 the most suitable for the prototype determined. The slot-pole combination to be selected can vary and the selected value affects the design in different ways.

2.4. Winding Layer

Winding layer refers to the coil surface per slot. It can be used as two types. It is called single and double layer winding model. If the winding is made so that two different coil sides per slot are made, it is called double layer winding, if there is one coil side per slot, it is called single layer winding [14].

2.4.1. Single layer winding

All conductors in this winding type in slot are connected in series with coils in the other slot to form a single-layer winding. The number of coils is half a half compared to the double layer type. There is no need for isolation between layers. Therefore, slot fill factor may be higher. It is widely used in small capacity machines. An example of a 3-phase stator with 36 slots of a single-layer winding is shown in Figure 5 [14].
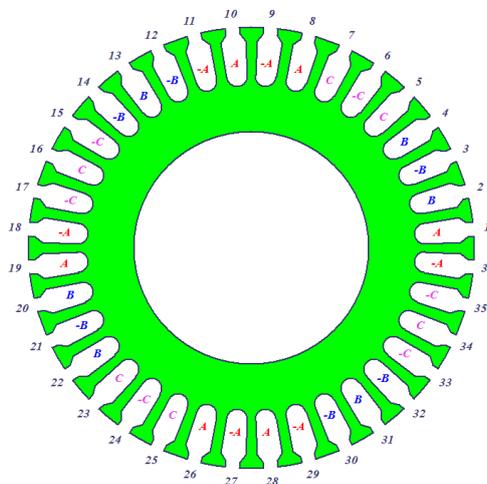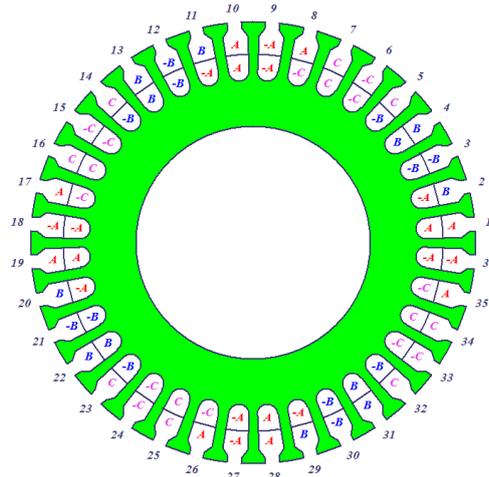

Figure 5. Single layer winding.

2.4.2. Double layer winding

In this winding-type, in slot there are two layers called lower and upper. One side of each coil is embedded in a slot on the lower side and the other on the upper side in another slot. The number of coils is doubled according to the single layer winding type. Since the insulation material is placed between the layers, the slot fill factor is lower. The electrical stress between phases is higher. It is used in high power applications. An example of a 3-phase stator with 36 slots of double-layer winding is given in Figure 6, [14].

Figure 6. Double layer winding.

2.5. Coil Connection Type

The coil connection is made in two different ways. These types of connections are called Whole Coiled and Half Coiled [15].

2.5.1. Whole coiled type

The motor windings represent the type of connection to occur as the connection of a plurality of coils per phase corresponding to the poles. This type of winding is called the Whole Coiled Type and shown in Figure 7 [15].
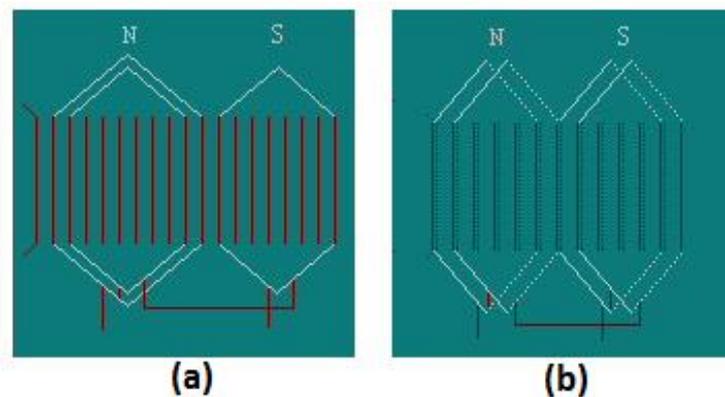
Figure 7. Types of whole coiled according to layers
(a) Single layered, (b) Double layered.

2.5.2. Half coiled type

When the motor windings are connected, they represent the type of connection that will occur in the form of corresponding to only one coil per pole pair per phase. This type of winding is called Half Coiled Type and shown in Figure 8 [15].

A. S. Çağışlar, H. Tiryaki, N. Bayhan
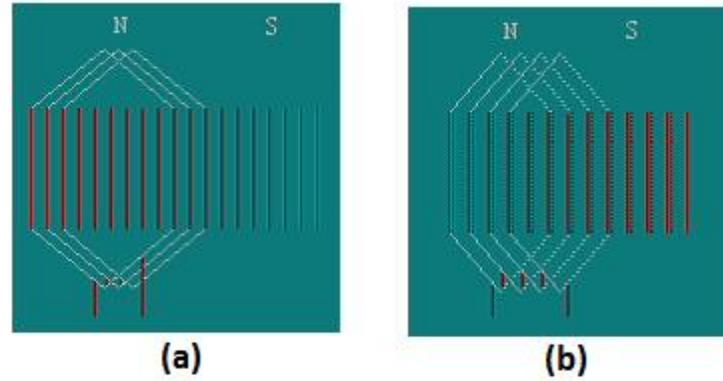
Figure 8. Types of half coiled according to layers
(a) Single layered, (b) Double layered.

2.6. Coil Range

The distance between the two sides of a coil of the motor winding is expressed as the coil spacing. The coil is called Full Range Coil (FRC) when the angular distance between the two sides of a coil is equal to the angular distance between adjacent field poles. The winding formed using FRC is called Full Range Winding.

If the number of coil spacing is less than the ratio of the total number of slots to the number of poles, the shorter coil spacing is called the longer coil spacing. The long coil range is used in variable speed applications. Furthermore, increasing the coil spacing will be more effective in terms of efficiency as it will produce eddy current in the larger area [15]. Figure 9 shows the motor windings with coil spacings 1, 2 and 3, respectively.
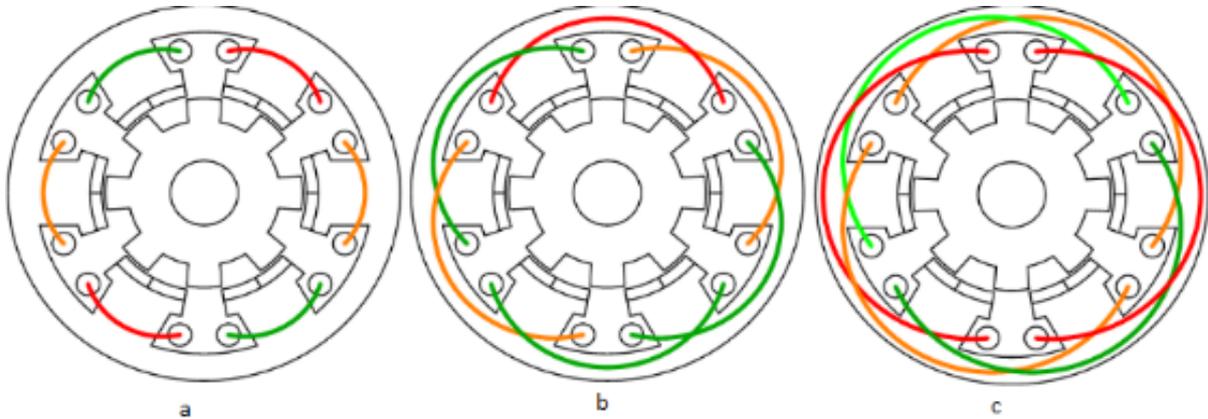
Figure 9. Winding ranges of motors (a) 1 spaced, (b) 2 spaced, (c) 3 spaced.

In the motor designs created using FRC, it has been seen in the literature studies that it has increased the inverse electromotive force and it has been seen that the motor efficiency is affected negatively by causing the vibration caused by the motor called cogging [16, 17].

2.7. Determination of Motor Dimensions and Structural Parameters

In terms of motor design, the location of the motor is the pioneer in determining many parameters such as stator and rotor dimensions of the motor, determination of slot-pole combination and magnet dimensions.

The dimensions to be chosen here are determined according to the space behind the wheel in AZAK vehicle. These dimensions of the motor are composed of stator and rotor.

EFFECTS OF NUMBER OF TURNS OF ARMATURE WINDING ON OUTER ROTOR BRUSHLESS DIRECT CURRENT MOTOR DESIGNED FOR AN ELECTRIC VEHICLE PROTOTYPE

2.7.1. Stator parameters

The dimensions of the stator of the motor and the properties of the materials in the stator part are given in Table 4.

Table 4. Stator features [1]

Features	Values/Types
Outer Radius	*240 mm*
Inner Radius	*180 mm*
Width	*30 mm*
Sheet Type	*Steel_1010*
Stacking Factor	*0.95*
Tilt Width	*0*

The inclination width represents the slope of the stator slots. With this feature, different designs are provided. At the design stage, this value will be 0 and there will be no slope.

Figure 10 shows the laminated ferromagnetic material. The stacking factor range, which is also found in the stator parameters, is typically chosen in the range of 0.8 to 0.99 [1].
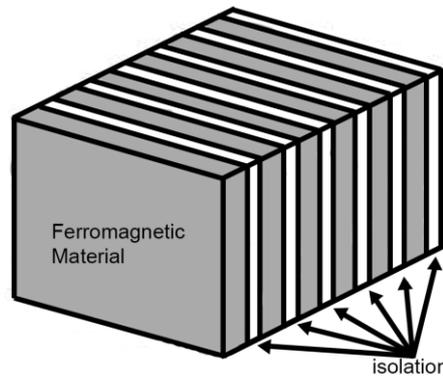
Figure 10. Laminated ferromagnetic material.

The parameters determined when we consider the motor's winding type are shown in Table 5.

Table 5. Winding parameters

Features	Values/Types
Winding Layer	*2*
Connection Type	*Half Coiled*
Parallel Winding Nr.	*1*
Coil Range	*1*
Slot Occupancy Ratio	*0.6*

The value referred to as coil spacing indicates that the next conductor wire of a coil will come out of the slot. The slot fill factor gives the ratio of the volume of conductive and insulating materials in a slot to the volume of the entire slot.

2.7.2. Rotor parameters

The dimensions of the rotor of the motor that is designed as an outer rotor and the information contained in the rotor part are given in Table 6.

The metal material used to reduce the effect of eddy currents is laminated as thin as possible and covered with insulating material. The flow permeability of the material is not lost here, but the eddy currents that will occur are reduced. The stacking factor refers to the loss of lamination resulting from the material when calculating the flux of the material. It is available from

A. S. Çağışlar, H. Tiryaki, N. Bayhan

the manufacturer's catalogs. This factor in stator sheet metal produced by lamination method is considered to be 1 for the rotor planned to be made from one piece [18].

Table 6. Rotor features [1]

Features	Values/Types
Outer Radius	*260 mm*
Inner Radius	*244 mm*
Width	*30 mm*
Sheet Type	*Steel_1010*
Stacking Factor	*1*
Pole Frequency	*0.96*
Magnet Type	*N45-M*
Magnet Thickness	*2.8 mm*

Pole frequency often encountered in polar design is the value indicating how often the magnets to be placed on the rotor are placed in the rotor frame.

3. NUMERICAL RESULTS AND DISCUSSION

Finite element method is an emerging technique to solve the problems expressed by partial differential equations. This method which takes place in the field of engineering in the solution of these problems day by day is biomechanical, heat transfer, stress, electromagnetic, aerodynamic and so on are used in many areas.

The analysis of the parameters with the parameters will be carried out by ANSYS Maxwell Electromagnetics Suite 16.0.0 [19]. The results of this method will be examined.

In the analyses to be performed, the speed will be targeted and the design analysis for the determined speed value will be examined. The most effective factor on the basis of design is the number of turns properties will be examined and the differences in motor design against these features will be examined. In order to perform objective evaluation, all other parameters except this important parameters will be kept constant as shown above [20].

3.1. Effects of Number of Turns of Armature Winding

In this section, the results will be examined by changing the number of turns of armature winding around the specified number. In order to make an objective evaluation, the same values were used for all parameters except number of turns of armature winding in each simulation and especially the working voltage was kept at 48 V and the wire diameter was kept constant at 1.29 mm. With corresponding turns of 10, 11, 12, 13, 14 effects will be determined.

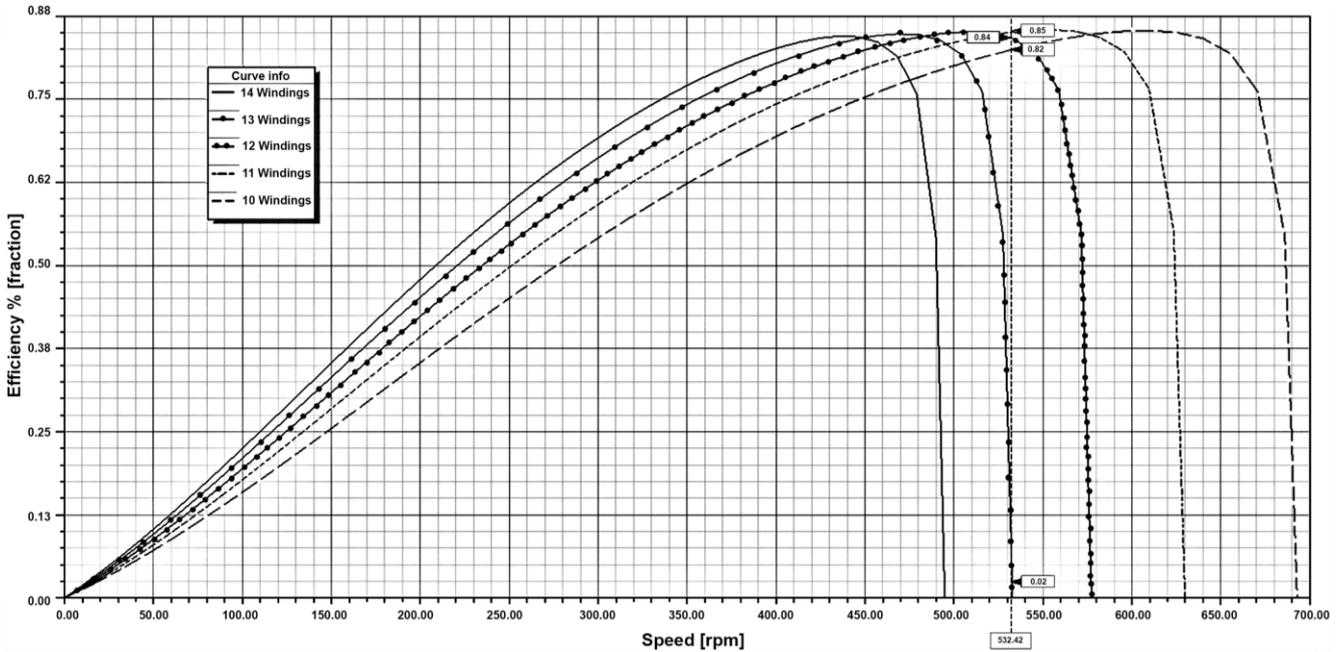### 3.1.1. Effect of number of turns of armature winding number to efficiency

When Figure 11 is examined, it is seen that the maximum speed value decreases with increasing number of turns of armature winding. From here it can be deduced that it is inversely proportional to the number of turns of armature winding. When the number of turns of armature winding is 12, the reference speed value is 532.42 rpm as indicated in Table 2. Table 7 shows the efficiency values corresponding to the number of turns of armature winding.

Table 7. Efficiency values corresponding to the number of turns of armature winding

Number of Turns of Armature Winding	10	11	12	13	14
Effciency Value (%)	82	85	84	2	-

When the efficiency value corresponding to the 13 turns design is examined in Table 7, it is observed that it is 0.02. This value cannot be considered as a suitable value for design. When the efficiency-speed graph of the 14 turns design is examined in Figure 11, it is observed that the reference speed value is outside this graph.
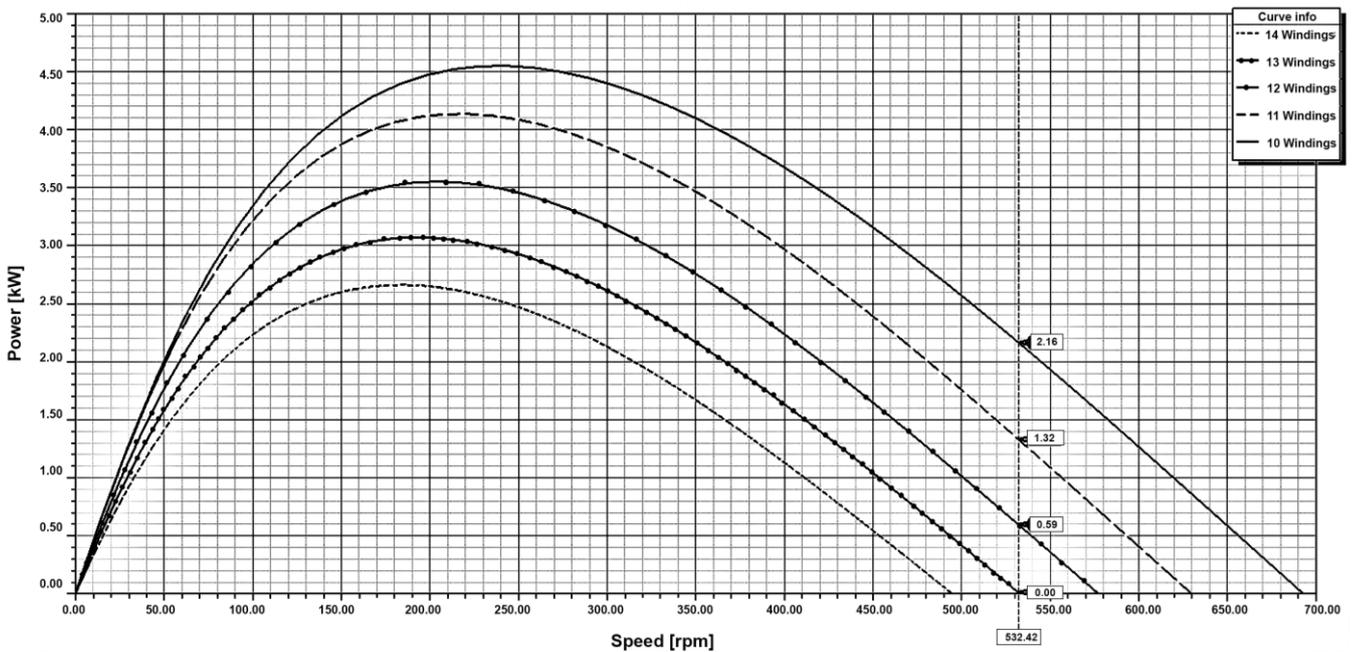
Figure 11. Effect of number of windings on efficiency-speed graph.

3.1.2. Effect of number of turns of armature winding to power

As shown in Figure 12, when the number of turns of armature winding is increased, it is observed that the power curve is reduced. According to the results obtained in the 12 turns design, the reference speed value is 532.42 rpm as indicated in Table 2 and the corresponding value for the specified speed value was 590 W. It is seen that it is met with a value close to the calculated design value of power indicated in Table 2.

Figure 12. Effect of number of turns of armature winding on power-speed graph.

A. S. Çağışlar, H. Tiryaki, N. Bayhan

Table 8 shows the power values corresponding to the number of turns for the reference speed value of 532.42 rpm.

Table 8. Power values corresponding to the number of turns of armature winding

Number of Turns of Armature Winding	10	11	12	13	14
Power (kW)	2.16	1.32	0.59	0	-

As shown in Table 8, with these values 13 and 14 turns designs were not suitable for prototype. In addition, when the power-speed graph of 14 turns design is examined in Figure 12, it is observed that the reference speed value is outside this graph.

3.1.3. Effect of number of turns of armature winding to torque

As shown in Figure 13, it is observed that the number of turns of armature winding decreases when the same speed value is taken into consideration and the torque value decreases. In Table 2, the specified torque value for 532.42 rpm is shown as 9.2 Nm. Referring to the graph in Figure 13, the torque value corresponding to the 12 turns design is shown in Table 9 to 10.56 Nm. In addition, when the torque-speed graph of 14 turns design is examined in Figure 13, it is observed that the reference speed value is outside this graph.

Figure 13. Effect of number of turns of armature winding on torque-speed graph.

Table 9 shows the torque values corresponding to the number of turns of armature winding for the reference speed value 532.42 rpm.
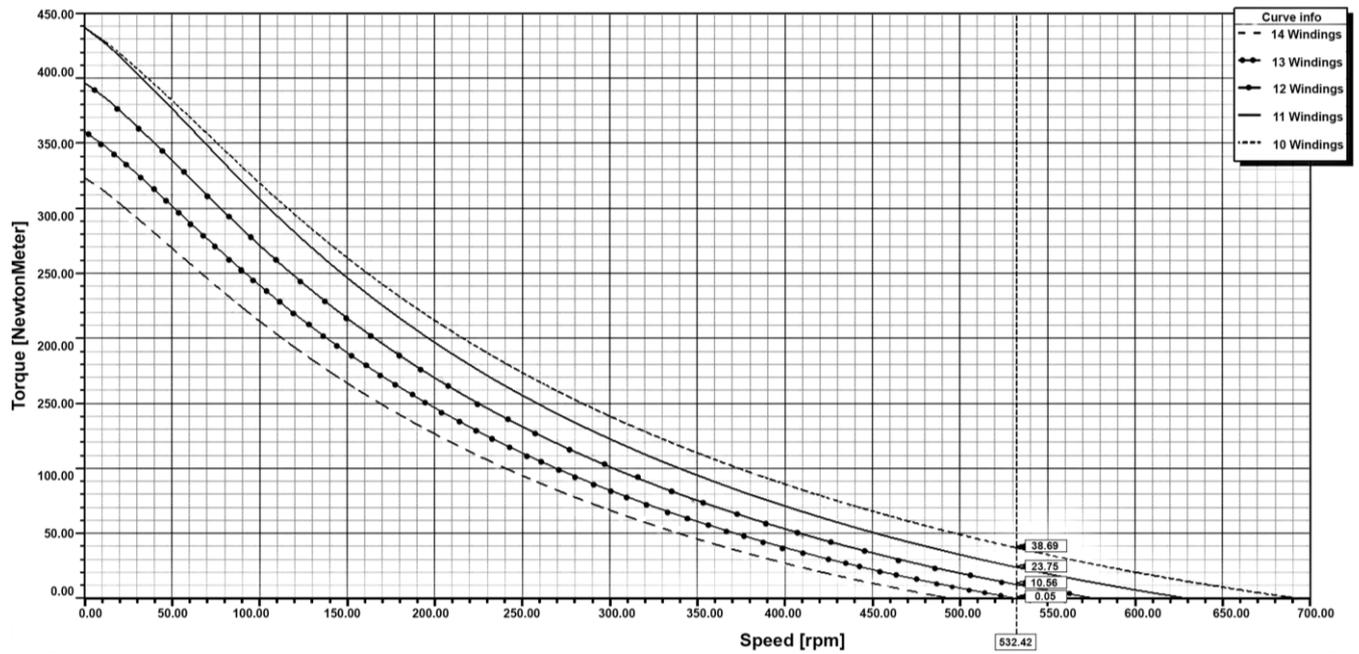
Table 9. Torque values corresponding to the number of turns of armature winding.

Number of Turns of Armature Winding	10	11	12	13	14
Torque (Nm)	38.69	23.75	10.56	0.05	-

As shown in Table 9, the torque value corresponding to the 12 turns design is shown in Table 9 to 10.56 Nm.

EFFECTS OF NUMBER OF TURNS OF ARMATURE WINDING ON OUTER ROTOR BRUSHLESS DIRECT CURRENT MOTOR DESIGNED FOR AN ELECTRIC VEHICLE PROTOTYPE

3.1.4. Magnetic and electrical effects of number of turns of armature winding

When the number of turns of armature winding is taken into account when analyzing the design, the change of this parameter affects many parameters in the analysis.

While examining the effects of the number of turns of armature winding in this section, the parameters of Armature Current Density, Copper Losses and Average Input Current will be examined. Armature Current Density refers to the ratio of the current flowing through the unit area on the luminaire. In the literature, it is observed that the heat density on the luminaire increases if this value is high. It is known that keeping the internal temperature of the motor low, as well as increasing the efficiency, will increase the motor efficiency and provide a more useful motor design [21].

$$\rho = \frac{RA}{l} \tag{11}$$

The expression of the self-resistance of the material is given in (11). ρ is self resistance and the unit is ohm-meter. R is the resistance, A is the cross section and l is the length of the material. The current capacity of the wire depends on the cross-sectional area and the thermal environment. The expression that the heat density in a resistor is I^2R is equal to the expression ρJ^2 where J is the current density. According to experience and studies, current density should be between 1 and 10 A/mm^2 [1].

The main factors affecting copper losses are the flow through the copper and the total resistance of the copper through which it flows. The analysis values corresponding to the change in the number of turns of armature winding in the light of all this information are shown in Table 10.

Table 10. Armature current density, copper losses and input current according to the number of turns of armature winding

Number of Turns of Armature Winding	Armature Current Density (A/mm^2)	Copper Losses (W)	Average Input Current (A)	Effciency Value (%)
10	9.4	198.71	51.74	82
11	5.07	63.70	29.82	85
12	2.10	10.58	12.25	84
13	0.45	0.47	-0.72	2
14	2.97	19.63	-10.86	-

As shown in Table 10, the flow values of the 13 and 14 turns designs were found to be less than 0. This means that the designs corresponding to the number of turns of armature winding are considered inappropriate. Turns 10 and 11 designs were not preferred because they had a negative effect on the design of the motor.

3.1.5. Flux densities

The space between the teeth and the rotor and the stator is called the air gap. The flux density in this area is considered as a research topic in itself. As a result of the studies carried out, the value of the flux density in this area, the value of an external magnetic field and the permanent point of the magnets acts as a magnetic field. The flux density in the air gap causes an impact that causes vibrations, which leads to vibrations called cogging and reduces motor performance. Figure 14 shows the magnetic flux densities of the motor generated according to the design parameters determined.

NÖHÜ Müh. Bilim. Derg. / NOHU J. Eng. Sci. 9(2): 832-847

A. S. Çağışlar, H. Tiryaki, N. Bayhan
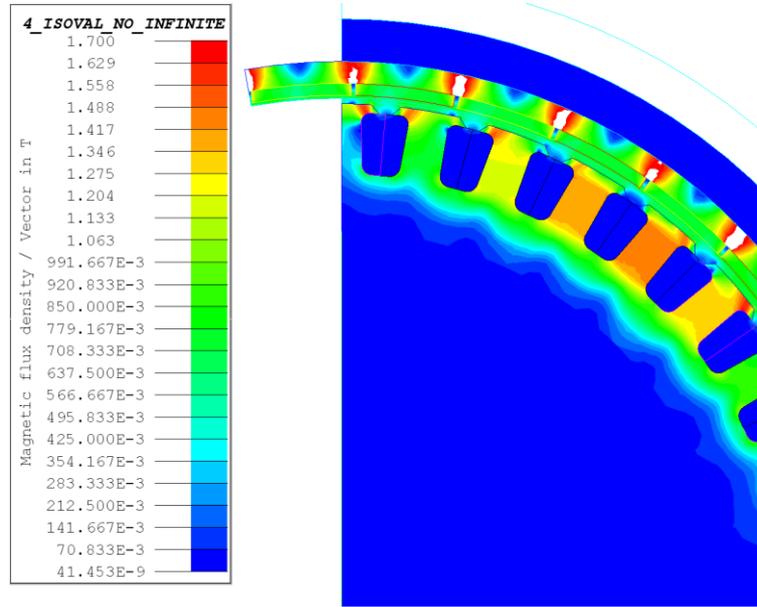
Figure 14. Display of magnetic flux densities [22].

When considering the flux density on the stator, there should be stator teeth since the place to be observed is exposed to more flux density than the area per unit. This case increases the importance of the selection of the correct number of turns of armature winding.
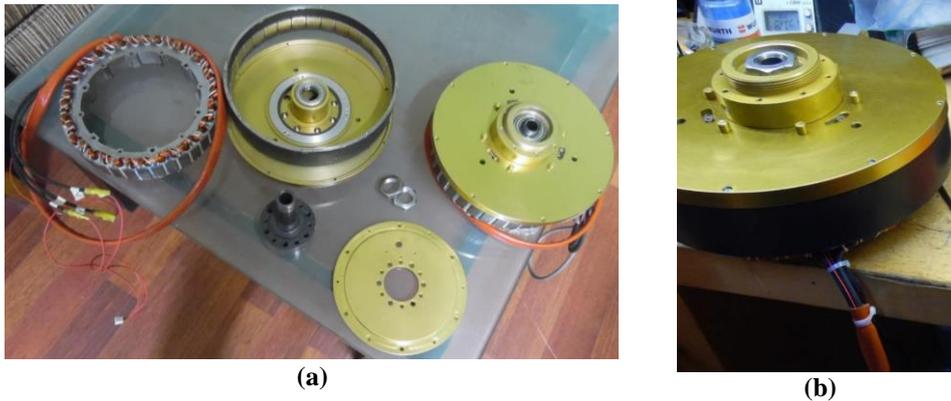
3.1.6. Transition to production

As a result of the analysis studies carried out for the design, the mechanical drawings shown in Figure 15 were made in order to produce the motor.

(a)

(b)
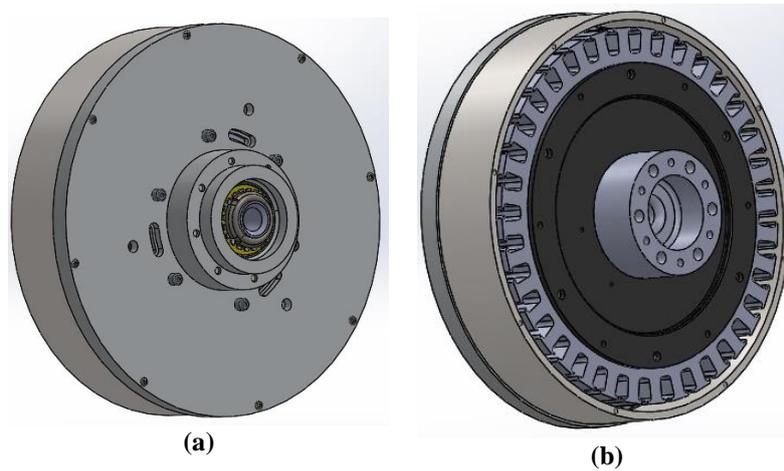
Figure 15. Mechanical drawings used for transition to production
(a) Rotor side, (b) Stator side.

It was decided to use the mechanical drawings shown in Figure 15 for the transition to production. After the completion of the production studies, the images of the motor designed in this study are presented in Figure 16.

EFFECTS OF NUMBER OF TURNS OF ARMATURE WINDING ON OUTER ROTOR BRUSHLESS DIRECT CURRENT MOTOR DESIGNED FOR AN ELECTRIC VEHICLE PROTOTYPE

(a)   (b)

Figure 16. Mechanical drawings used for transition to production
(a) Rotor side, (b) Stator side.

The motor shown in Figure 16 is used without any problems for Alternative Energy Vehicle Races organized by the TUBITAK in electric vehicle prototypes of MilAT 1453 R&D Society of Istanbul University - Cerrahpaşa.

4. CONCLUSION

In the electric vehicle prototypes, direct drive brushless direct current motors are desired because of their higher efficiency. However, with a purpose to preserve effectivity in the highest variety, the motors have to be designed and manufactured in response to the vehicle and its elements. It is vitally fundamental to determine the right quantity of turns of armature winding, as well as many parameters for the period of the design segment. It is rather major to examine all motor parameters targeted to the vehicle to which the motor might be applied in the course of the design segment.

In this study, the design parameters determined according to the physical, electrical and magnetic constraints of the motor, which constitute the design input parameters, were obtained. These parameters include a number of substances, such as values and physical measurements, determined by the aerodynamic analysis of the vehicle to be used. In order to calculate the input parameters of the motor which is designed in the light of these values, necessary information has been realized with the help of many articles and academic studies.

The study includes the design of the BLDC motor for the electric vehicle prototypes. In addition, the effects of the number of turns of armature winding on the design were analyzed in detail. As a result of these investigations, it was concluded that the optimum number of turns of armature winding is 12 for the motor design.

In the near future, it is planned to start the production from the motor design and to make analyzes based on experimental results and to contribute to the literature.

ACKNOWLEDGMENTS

REFERENCES

[1] D. Hanselman, Brushless Permanent Magnet Motor Design, Magna Physics Publishing, 9nd ed. ISBN: 1-881855-15-5, Lebanon, 2003.

[2] P. Yedemale, "Brushless DC (BLDC) Motor Fundamentals", Microchip Technology Inc, App. Note: DS00885A, pp. 1-20, USA, 2003.

[3] M.R.A. Pahlavani, Y.S. Ayat and A. Vahedi, "Minimisation of torque ripple in slotless axial flux BLDC motors in terms of design considerations", *IET Electric Power Applications*, vol.11, no.6, pp. 1124-1130, 2017.

[4] N. A. Rahim, H. W. Ping and M. Tadjuddin, "Design of Axial Flux Permanent Magnet Brushless DC Motor for Direct Drive of Electric Vehicle", Proc. 2007 IEEE Power Engineering Society General Meeting, Tampa, FL, USA, 2007.

A. S. Çağışlar, H. Tiryaki, N. Bayhan

[5] N. Shrivastava and A. Brahmin, "Design of 3-Phase BLDC Motor for Electric Vehicle Application by Using Finite Element Simulation", *International Journal of Emerging Technology and Advanced Engineering*, vol. 4, no. 1, pp. 140–145, 2014.

[6] D. Uygun and S. Solmaz, "Design and Dynamic Study of a 6 kW External Rotor Permanent Magnet Brushless DC Motor for Electric Drivetrains", Proc. 2015 IEEE 5th International Conference on Power Engineering, Energy and Electrical Drives (POWERENG), Riga, Latvia, 2015.

[7] H. Tiryaki, A. Akgundoğdu, G. Erdogan, O. Karadeniz, U. Sahin, M.Y. Yılmaz, Y. Durak and I. Kocaarslan, "Implementation of an Electromobile for Efficiency Challenge", Proc. Int. World Electro Mobility Conference (WELMO'17), Izmir, Turkey, 2017. (In Turkish)

[8] Car Acceleration, Available: https://www.engineeringtoolbox.com/car-acceleration-d_1309.html [Accessed: Sept. 03, 2019].

[9] M. Jafarboland and M.M. Sargazi, "Analytical modelling of the effect of pole offset on the output parameters of BLDC motor", *IET Electric Power Applications*, vol.12, no.5, pp.666-676, 2018.

[10] Y. Luo, Y. Zhu, Y. Yu and L. Zhang, "Inductance and force calculations of circular coils with parallel axes shielded by a cuboid of high permeability", *IET Electric Power Applications*, vol.12, no.5, pp.717-727, 2018.

[11] F. Libert and J. Soulard, "Investigation on Pole-Slot Combinations for Permanent-Magnet Machines with Concentrated Windings", Proc. Int. Conf. on Electric Machines (ICEM'04), 2004.

[12] A.S. Cabuk, Ş. Sağlam, G. Tosun and O. Ustun, "Investigation of Different Slot-Pole Combinations of An In-Wheel BLDC Motor for Light Electric Vehicle Propulsion", Proc. Int. Conf. on ELECO'17, 2017.

[13] C. Ma, Q. Li, H. Lu H, Y. Liu and H. Gao, "Analytical model for armature reaction of outer rotor brushless permanent magnet DC motor", *IET Electric Power Applications*, vol.12, no.5, pp.651-657, 2018.

[14] P. Kohnke, ANSYS Theory Reference for The Mechanical APDL and Mechanical Applications, SAS IP, Canonsburg, 2009.

[15] P.M. Dusane, Simulation of a Brushless DC Motor in ANSYS – Maxwell 3D, Master Thesis, Czech Technical University, 2016.

[16] W. Fei and P.C.K. Luk, "A New Technique of Cogging Torque Suppression in Direct-Drive Permanent Magnet Brushless Machines", *IEEE Transactions on Industry Applications*, vol.46, no.4, pp.1332-1340, 2010.

[17] Z. Wu and Z.Q. Zhu, "Influence of stator/rotor-pole combination on electromagnetic performance in all/alternate poles wound partitioned stator doubly salient permanent magnet machines", *J Eng*, vol.6, pp.237–245, 2017.

[18] Stacking Factor, Available: https://en.wikipedia.org/wiki/Stacking_factor, [Accessed Sept. 03, 2019].

[19] ANSYS Maxwell Electromagnetics Suite 16.0.0, Reference Manual, 2015.

[20] A.S. Çağışlar, Brushless Direct Current Motor Design For Electric Vehicles, Master Thesis, Istanbul University, 2018. (In Turkish)

[21] L. Tang, J. He, L. Chen, S. Xia, D. Feng, J. Li and P. Yan, "Study of Some Influencing Factors of Armature Current Distribution at Current Ramp-Up Stage in Railgun", *IEEE Transactions On Plasma Science*, vol.43, no.5, pp.1585-1591, 2015.

[22] Flux, Reference Manual, 2018.